The Plant Cell, Vol. 23: 1932–1944, May 2011, www.plantcell.org

Identification of an *Arabidopsis* Plasma Membrane–Located ATP Transporter Important for Anther Development [W]

Benjamin Rieder and H. Ekkehard Neuhaus[1]

Plant Physiology, Technical University of Kaiserslautern, D-67653 Kaiserslautern, Germany

ATP acts as an extracellular signal molecule in plants. However, the nature of the mechanisms that export this compound into the apoplast are under debate. We identified the protein PM-ANT1 as a candidate transporter able to mediate ATP export. PM-ANT1 joins the mitochondrial carrier family, lacks an N-terminal amino acid extension required for organelle localization, and locates to the plasma membrane. Recombinant PM-ANT1 transports ATP, and the gene is substantially expressed in mature pollen grains. Artificial microRNA (amiRNA) mutants show reduced silique length and less seeds per silique but increased seed weight associated with unchanged pollen viability. Anthers from amiRNA mutants exhibited a normal early development, but stomium breakage is inhibited, leading to impaired anther dehiscence. This results in reduced self-pollination and thus decreased fertilization efficiency. amiRNA pollen grains showed increased intracellular ATP levels but decreased extracellular ATP levels. The latter effects are in line with transport properties of recombinant PM-ANT1, supporting in planta that functional PM-ANT1 resides in the plasma membrane and concur with the *PM-ANT1* expression pattern. We assume that PM-ANT1 contributes to ATP export during pollen maturation. ATP export may serve as an extracellular signal required for anther dehiscence and is a novel factor critical for pollination and autogamy.

INTRODUCTION

Nucleotides represent the universal cellular energy currency in all living cells and act as core components for all forms of viral, bacterial, and eukaryotic genetic information building our nucleic acid world. Thus, the presence of these molecules can be taken as proof for the presence of life itself. Moreover, these types of molecules and derivatives act as cofactors for many enzymes, as secondary messengers in intracellular signaling cascades, and as biosynthetic precursors of a wide diversity of cellular polymers.

Interestingly, ATP itself serves as an intra- and extracellular signaling molecule. For instance, the cellular energy status is sensed by a Snf-kinase measuring the cytosolic ATP/AMP ratio (Hardie et al., 1998). By this mechanism, alterations of cell type–specific ATP/AMP ratios are received and induce metabolic adaptation balancing cellular energy provision. In yeast and mammals, and most prominently analyzed in humans, ATP acts in addition as an extracellular signaling molecule that interacts with the so-called P2 purinoreceptors, representing membrane-bound proteins. By this mechanism, ATP functions as an important neurotransmitter both in the central and peripheral nervous systems (Bodin and Burnstock, 2001b). In addition, after perception of extracellular ATP, a signal cascade is activated that is inter alia involved in blood pressure regulation, cancer tumor growth, or fitness of immune cells (Pellegatti et al., 2008; Trautmann, 2009; Stagg and Smyth, 2010).

[1] Address correspondence to neuhaus@rhrk.uni-kl.de.
The author responsible for distribution of materials integral to the findings presented in this article in accordance with the policy described in the Instructions for Authors (www.plantcell.org) is: H. Ekkehard Neuhaus (neuhaus@rhrk.uni-kl.de).
[W] Online version contains Web-only data.
www.plantcell.org/cgi/doi/10.1105/tpc.111.084574

Remarkably, detailed recent work showed that the plant apoplastic fluid contains ATP, and the extracellular presence of this metabolite is perceived by so far uncharacterized receptor proteins (Kim et al., 2006; Roux and Steinebrunner, 2007). By use of apoplastic apyrase expressing mutants, which show reduced extracellular ATP levels, or by feeding of extracellular ATP, it was possible to identify processes like apoptosis, pathogen defense, cell cycle, and root gravitropism as being regulated by this primary metabolite (Steinebrunner et al., 2003; Tang et al., 2003; Song et al., 2006; Roux and Steinebrunner, 2007). In addition to ATP, NAD^+ has also been identified as an extracellular signaling molecule in plants (Zhang and Mou, 2009).

There is evidence that in animals, cellular ATP export occurs by vesicle fusion with the plasma membrane (Bodin and Burnstock, 2001a). This observation is in line with properties of the vesicular H^+/ATP antiporter VNUT, which imports ATP against a concentration gradient and leads to nucleotide-filled vesicles primed to fuse with the plasma membrane (Sawada et al., 2008). In addition, channel proteins and plasma membrane–located ABC transporters have been proposed to function as ATP export proteins (Bodin and Burnstock, 2001b; Dutta et al., 2002; Lazarowski et al., 2003). However, both an ABC transporter named PGP1 and exocytosis have been proposed to mediate ATP release by plant cells (Thomas et al., 2000; Kim et al., 2006). ATP transport by these mechanisms has not been studied in detail (e.g., little is known about substrate specificity, apparent affinities, or driving energy).

Oxidative mitochondrial metabolism and associated nucleotide transport processes have been deciphered in considerable detail (Klingenberg, 2008), but our understanding of nucleotide transport across other cellular membranes is merely emerging. In plants, two types of nucleotide transporters have been identified

on the molecular level, namely, NTT-type and mitochondrial carrier family (MCF)–type carriers. Nucleotide transporters of the NTT type are phylogenetically derived from bacterial homologs (Kampfenkel et al., 1995; Schmitz-Esser et al., 2004), reside in all forms of plastids, and are responsible for ATP import into chloroplasts during the night (Reinhold et al., 2007) or into heterotrophic plastids to energize anabolic reactions (Neuhaus et al., 1993a, 1993b; Tjaden et al., 1998a). In *Arabidopsis thaliana*, two NTT isoforms exist, and both localize to plastids and show tissue-specific expression patterns (Möhlmann et al., 1998; Reiser et al., 2004). The second type of plant ATP carrier belongs to the large MCF and consists of a subgroup of putatively orthologous genes (Millar and Heazlewood, 2003). Interestingly, MCF-type ATP carriers are not restricted to mitochondria but are also present in peroxisomes and glyoxysomes (Arai et al., 2008; Linka et al., 2008) and in the endoplasmic reticulum (ER) (Leroch et al., 2008). However, there are further candidate ATP transporters in the mitochondrial carrier family with unknown subcellular location, uncharacterized transport properties, and nonidentified cellular impact.

Accordingly, we started a rigorous analysis of the function of further putative ATP carriers and identified PM-ANT1 as a candidate carrier able to export ATP from the plant cell. In line with transport characteristics and the specificity of *PM-ANT1* gene expression, we identified a critical function of this carrier in anther development and autogamy. We provide evidence that extracellular ATP fulfils a novel plant-specific function, namely, the intercellular signaling required for communication between mature pollen grains and the anther tapetum.

RESULTS

Amino Acid Sequence of PM-ANT1

The *Arabidopsis* genome encodes 58 predicted MCF-type carrier proteins, and a phylogenetic analysis classified PM-ANT1 as a member of the MCF, forming a monophyletic subcluster with the three mitochondrial ADP/ATP carriers AAC1-3 (Picault et al., 2004). Within this subcluster, PM-ANT1 shows highest structural identity with the ER-located ATP/ADP carrier ER-ANT1 (33% identity; 53% similarity) followed by the mitochondrial protein AAC1 (30% identity; 48% similarity).

The sequence of PM-ANT1 consists of 330 amino acids exhibiting three tandem repeats of ~100 residues and six predicted transmembrane helices (Figure 1). Both the presence of three tandem repeats and three conserved mitochondrial energy transfer signatures (METS) in PM-ANT1 (Figure 1) are characteristic features of all MCF-type carriers (Saraste and Walker, 1982; Palmieri et al., 2011). Similar to the ER-located ATP/ADP carrier ER-ANT1, but in contrast with the mitochondrial proteins AAC1, AAC2, and AAC3, PM-ANT1 does not possess a putative N-terminal transit peptide (Figure 1). However, such sequence extension in plant AAC proteins is strictly required for targeting to the inner mitochondrial membrane (Murcha et al., 2005).

A comprehensive study of amino acids essential for the function of mitochondrial AACs suggests a putative biochemical function for PM-ANT1 as an ATP/ADP transporter. For example, the presence of a so-called nucleotide carrier signature consisting of the amino acid sequence RRRMMM is a unique signature for all MCF-type ATP/ADP carriers like AAC1-3 and ER-ANT1 (Leroch et al., 2008; Palmieri et al., 2011) and is also present in PM-ANT1 with the first Met replaced by the structurally related Ile residue (Figure 1). However, the three Arg residues in the nucleotide carrier signature are only part of in total six Arg residues (Arg-107, Arg-215, Arg-264, Arg-265, Arg-266, and Arg-307) found to be crucial for the ADP/ATP transport activity of the yeast AAC2 protein (Nelson et al., 1993). Furthermore, the structure of the bovine AAC1 monomer was solved at a resolution of 2.2 Å by x-ray crystallography (Pebay-Peyroula et al., 2003). Several clusters of charged amino acids were identified as being potentially involved in substrate binding and therefore are fundamental for the function of mitochondrial AACs. In the translocation channel of bovine AAC1, a cationic cluster consisting of two Lys and six Arg residues (Lys-22, Lys-32, Arg-79, Arg-137, Arg-234, Arg-235, Arg-236, and Arg-279) directed to the substrate was identified. The positions of their side chains were stabilized by an intricate hydrogen bond network and electrostatic interactions involving water molecules and acidic or polar side chains of Glu-29, Asp-134, Asp-231, Gln-36, Glu-264, and Asn-276. Most of these important charged or polar amino acids are conserved in PM-ANT1, namely, Lys-55, Arg-107, Arg-215, Arg-264, Arg-265, Arg-266, and Arg-307 and Glu-52, Asp-163, Asp-263, Gln-59, Glu-292, and Asn-304, but the basic amino acid Lys-22 is replaced by the basic amino acid His-45 (Figure 1). In summary, the high conservation of amino acid residues critical for the function of mitochondrial AACs indicates a function for PM-ANT1 as an adenylate transport protein.

Functional Expression of PM-ANT1 in *Escherichia coli*

We tried to synthesize recombinant PM-ANT1 in yeast or *Xenopus laevis* oocytes. After expression of *PM-ANT1* constructs, the corresponding cells were incubated for different periods of time in radioactively labeled ATP, but no net uptake above the background was detectable. However, it has frequently been shown that heterologous synthesis of other nucleotide transporters (e.g., the three plant mitochondrial AACs, the ER-located ATP/ADP carrier ER-ANT1 from *Arabidopsis*, and various plant-derived NTT-type ATP carriers in *E. coli*) lead to their functional integration into the bacterial cytoplasmic membrane, with transport properties similar to those obtained across the authentic membranes (Haferkamp et al., 2002; Leroch et al., 2008; Tjaden et al., 1998a; Ast et al., 2009). Heterologous synthesis of PM-ANT1 in *E. coli* also results in the integration of this carrier into the bacterial membrane because after isopropyl-β-D-thiogalactopyranoside (IPTG) induction, a substantial fraction of the recombinantly synthesized PM-ANT1 migrated according to the calculated molecular mass of ~36.9 kD (Figures 2A and 2B).

Uptake studies with radioactively labeled [α-^{32}P]ATP or [α-^{32}P]ADP into intact bacterial cells harboring PM-ANT1 revealed the time-linear import of both nucleotides for ~5 min, whereas, by contrast, noninduced *E. coli* cells hardly imported adenylates (Figure 2C). The import of radioactively labeled ATP or ADP by recombinant PM-ANT1 into *E. coli* cells displayed typical Michaelis-Menten kinetics with apparent K_m values of 284 μM

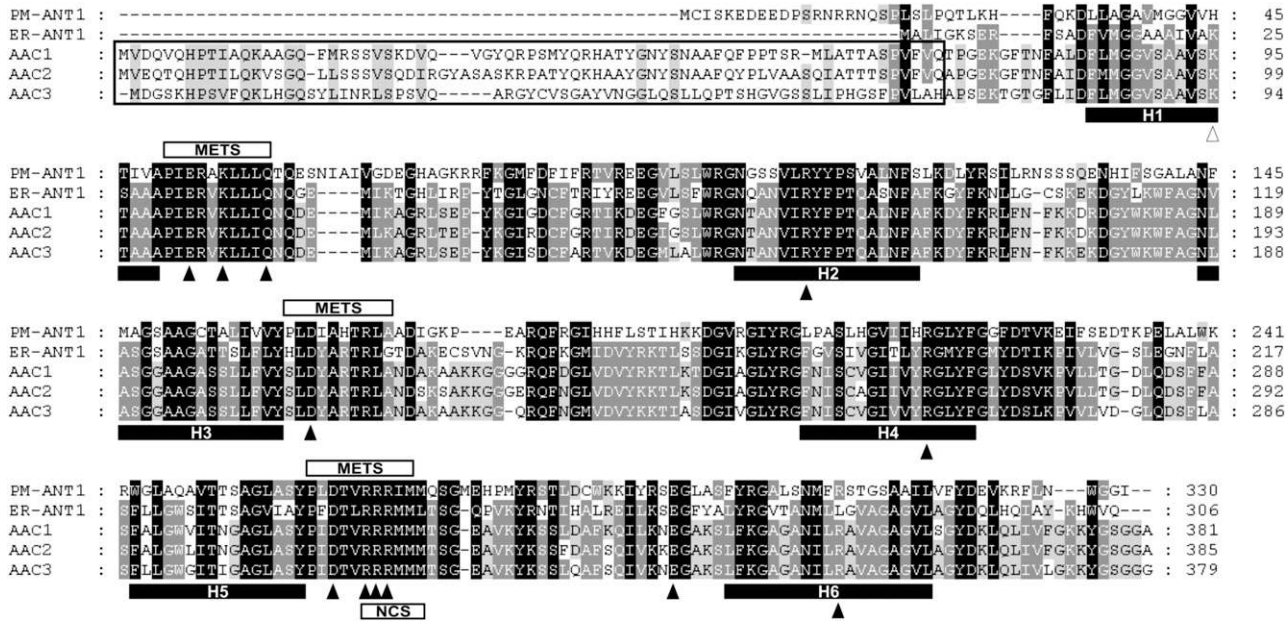

Figure 1. Alignment of the Predicted Amino Acid Sequence of PM-ANT1 with Those of ER-ANT1 and AAC1-3 from *Arabidopsis*.

The amino acid residues identical or similar among all family members are shaded in black, conserved residues in four proteins are shaded in gray, and conserved residues in three proteins are shaded in light gray. The predicted N-terminal mitochondrial transit peptides of AAC1 to AAC3 are indicated by black squares. Solid black bars underline six putative membrane-spanning regions (H1 to H6). The conserved METS (METS=P-x-[DE]-x-[LIVAT]-[RK]-x-[LRH]-[LIVMFY]-[QGAIVM]) following each odd membrane-spanning domain and the conserved nucleotide carrier signature (NCS) are marked by white bars. Triangles indicate important amino acid residues for the function of mitochondrial AACs (see text): black triangles represent amino acid residues conserved also in PM-ANT1, and white triangles indicate residues not conserved in PM-ANT1.

(±21.4 μM) for ATP (Figure 2D) and 422 μM (±38.1 μM) for ADP (Figure 2E). Competition experiments with 29 different potential substrates showed that PM-ANT1 is mainly inhibited by purine and pyrimidine (deoxy)trinuceotides but not by nicotine-amid dinucleotides or nucleotide sugar derivatives (Table 1). The uncoupler compound CCCP does not inhibit ATP uptake by PM-ANT1 (Table 1), indicating that transport is not energized by a proton motif force.

Subcellular Localization of PM-ANT1

The subcellular localization of PM-ANT1 was not predictable by the computer programs TargetP (Emanuelsson et al., 2000) and SignalP (Nielsen et al., 1997). Moreover, the lack of any putative plastidic or mitochondrial transit peptide (Figure 1) was confirmed by the use of the programs ChloroP and MitoProt (Claros and Vincens, 1996; Zybailov et al., 2008).

We investigated the subcellular localization of PM-ANT1 in planta by the generation of a PM-ANT1-green fluorescent protein (GFP) fusion and transient expression in intact tobacco (*Nicotiana tabacum*) protoplasts (Figure 3; note, most genes coding for membrane proteins are notoriously weakly expressed, making the use of a 35S cauliflower mosaic virus promoter for transient expression unavoidable). After expression of the constructed *PM-ANT1-GFP* gene, a fluorescence signal could be detected at the plasma membrane (Figure 3A). This conclusion about the subcellular localization is supported by the corresponding chloroplast autofluorescence (Figure 3B), the merged image (Figure 3C), and the colocalization of PM-ANT1-GFP and the plasma membrane–bound aquaporin fusion protein PIP2a-mcherry (see Supplemental Figure 1 online).

Expression Analyses of *PM-ANT1*

To study *PM-ANT1* gene expression in planta, we analyzed 14 independent *PM-ANT1-promoter-GUS* (for β-glucuronidase) *Arabidopsis* lines for reporter gene activity. Thirteen of these lines showed a very similar expression pattern, varying only slightly in the intensity of GUS staining.

In flowers, *PM-ANT1* gene expression is mainly visible in anther tissue and the style (Figure 4A). Pollen grains located on the stigma also show high *PM-ANT1* expression (Figure 4B) and young leaf veins, and the central cylinder from developing roots are also characterized for high *PM-ANT1* expression (Figures 4C and 4D). Relative *PM-ANT1* gene expression does not change during leaf development, and corresponding mRNA accumulation in roots is due to expression in proto- and meta-phloem (Genevestigator; Zimmermann et al., 2004). A closer examination of GUS staining in developing anthers revealed that this staining is in fact due to substantial *PM-ANT1* expression in pollen grains located inside the closed anther (Figure 4E). In siliques harboring developing seeds, *PM-ANT1* expression reached high levels and decreased to the lower sensitivity level during maturation of this organ (Figure 4F).

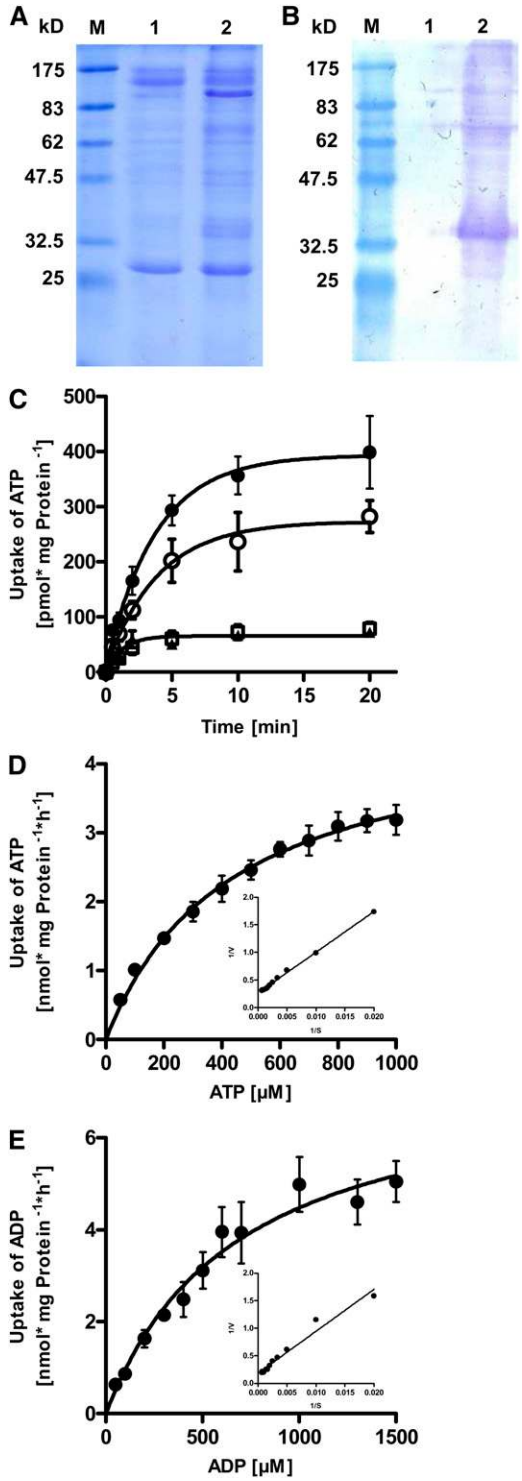

Figure 2. Analysis of Heterologously Expressed PM-ANT1 in *E. coli* Cells.

(A) and **(B)** SDS-PAGE of noninduced (lane 1) and IPTG-induced (lane 2) cells harboring the plasmid encoding PM-ANT1. Coomassie stained **(A)**; immunoblot **(B)**. M, marker showing molecular masses in kilodaltons.

(C) Time kinetics of adenine nucleotide uptake. IPTG-induced *E. coli* cells harboring the plasmid encoding PM-ANT1 were incubated with 200 μM [α-^{32}P]ATP (closed circles) or [α-^{32}P]ADP (open circles) for the indicated time intervals. Noninduced *E. coli* cells transformed with the plasmid encoding PM-ANT1 were used as controls (open triangles, ATP; open squares, ADP).

(D) Substrate dependency of ATP uptake.

(E) Substrate dependency of ADP uptake. Data are means ± SE of at least three independent experiments.

PM-ANT1 expression during pollen maturation was extracted from microarray experiments (Honys and Twell, 2004). In unicellular pollen, relative *PM-ANT1* transcription reached a value of ~125 and increased constantly during microgametogenesis. In mature pollen grains, *PM-ANT1* transcript was about fourfold above the level present at the beginning of pollen development (unicellular pollen) (see Supplemental Figure 2 online).

Generation of *PM-ANT1* Artificial MicroRNA Mutant Lines

To obtain insight into the physiological impact of PM-ANT1, we intended to make use of transgenic plants. Two independent heterozygous *PM-ANT1*::*T-DNA Arabidopsis* mutants carrying a T-DNA insertion either at the very end of the sole exon or at the beginning of the 3′-untranslated region, respectively, were provided by the SALK library (Alonso et al., 2003). After backcrossing, homozygous T-DNA lines were identified by PCR of genomic DNA; however, quantitative RT-PCR using *PM-ANT1*-specific primers exhibited an unchanged *PM-ANT1* transcript level in these mutants.

Thus, we decided to construct artificial microRNA (amiRNA) mutant lines. Selection of suitable DNA sequences was conducted according to Schwab et al. (2006) and http://wmd2.weigelworld.org. After transfer into the genome of wild-type plants, we were able to identify various independent *35S*:*amiRNA PM-ANT1* lines; most of them showed *PM-ANT1* mRNA levels similar to wild-type plants. However, by testing the *PM-ANT1* transcript level in ~100 independent mutants, we were able to identify, among others, the strong *35S*:*amiRNA PM-ANT1 PM-ANT1* lines 6 and 15. In these mutant lines, the *PM-ANT1* mRNA levels are reduced to ~26% in line 6 and to 23% in line 15 of wild-type levels (Figure 5A). To exclude unspecific effects on pollen grains due to the knockdown approach per se (Xing and Zachgo, 2007), we included *35S*:*amiRNA PM-ANT1* line 9 in our investigations. The latter mutant showed mRNA levels similar to wild-type plants (Figure 5A) and is thus expected to behave similarly.

After growing for 12 weeks in the climate-controlled growth chambers, a phenotypic difference between the strong *35S*:*amiRNA PM-ANT1* lines 6 and 15 and the wild-type line was obvious (Figure 5B). Both mutant lines showed significantly reduced numbers of fully developed siliques, whereas mutant line 9 exhibited silique development similar to wild-type plants (Figure 5B). The distorted silique development in mutant lines 6 and 15 correlated with decreased numbers of fully developed seeds (Figures 5C and 5D), whereas the control *35S*:*amiRNA PM-ANT1* line 9 and wild-type plants exhibited unaltered numbers of seeds per silique (Figures 5E and 5F).

Measurements of the average silique lengths allowed quantification of differences between wild-type and mutant lines.

Table 1. Effects of Various Metabolites on [α-^{32}P]ATP Transport by PM-ANT1

Effector	Transport Rate [%]
Control	100.0
ATP	57.9 (±2.4)
CTP	54.2 (±2.5)
GTP	54.0 (±3.2)
ITP	65.2 (±4.8)
UTP	53.9 (±1.2)
ADP	50.8 (±9.3)
GDP	85.9 (±2.7)
IDP	70.5 (±4.0)
UDP	79.7 (±8.8)
AMP	89.6 (±1.5)
CMP	99.0 (±5.2)
GMP	93.3 (±1.1)
IMP	87.5 (±2.6)
TMP	100.3 (±3.4)
UMP	92.2 (±1.5)
3′AMP	98.6 (±2.1)
dTTP	55.5 (±6.2)
dGTP	47.3 (±1.9)
dCTP	63.3 (±1.4)
dATP	50.7 (±0.2)
Ado	96.7 (±2.7)
ADP-Glc	74.6 (±8.5)
UDP-Glc	93.6 (±5.2)
NAD	98.6 (±6.9)
NADH	95.2 (±3.0)
NADP	94.7 (±9.7)
NADPH	96.2 (±1.6)
FAD	84.0 (±1.8)
CCCP	91.8 (±0.9)

Uptake in *E. coli* cells expressing PM-ANT1 was carried out for 2 min and stopped by rapid filtration (see Methods). ATP uptake was measured at a substrate concentration of 200 μM. Metabolic effectors were present in a 10-fold higher concentration than the substrate.

Wild-type plants and mutant line 9 showed average silique lengths of ~15 mm, whereas *35S*:*amiRNA PM-ANT1* lines 6 and 15 exhibited average silique lengths of only 6 and 9 mm, respectively (Figure 6A). Similarly, the average number of seeds per silique was similar in the wild type and weak *35S*:*amiRNA PM-ANT1* line 9 (between 56 to 64 seeds per silique), whereas *35S*:*amiRNA PM-ANT1* lines 6 and 15 exhibited significantly decreased seed numbers per silique, ranging from 11 seeds per silique in line 6 to 21 seeds per silique in line 15 (Figure 6B). Remarkably, the average seed weight appeared to be reciprocal to the number of seeds per silique. Both the wild type and *35S*:*amiRNA PM-ANT1* line 9 showed a 1000 seed weight of ~18 mg, whereas that of mutant line 15 was 24 mg and that of mutant line 6 was 33 mg (Figure 6C).

Segregation Analysis of *35S*:*amiRNA PM-ANT1* and Pollen Analysis

The observation that *35S*:*amiRNA PM-ANT1* lines exhibited fewer seeds per silique (Figures 5B and 6B) might indicate that mutant plants exhibit impaired male or female fertility. To control pollen fitness, we pollinated wild-type (+/+) stigma with pollen grains from heterozygous mutant lines 6 or 15 (+/line 6 or +/line 15). To test female gametophytic fertility, we pollinated the stigma from both heterozygous mutant lines with wild-type pollen grains. As controls, we allowed self-fertilization of the two heterozygous *35S*:*amiRNA PM-ANT1* lines 6 and 15. Genetic transmission efficiency was subsequently quantified by analyzing kanamycin resistance of successor seedlings, which is expected to cosegregate with *35S*:*amiRNA PM-ANT1* (see Supplemental Table 1 online).

Transfer of pollen from heterozygous mutant lines 6 and 15 to wild-type stigma led to 15 and 16 kanamycin-resistant seedlings, respectively, and 15 and 17 kanamycin-sensitive seedlings (see Supplemental Table 1 online). These numbers lead to 50 and 48.5%, respectively, antibiotic-resistant plants and can be taken as an indication that pollen fitness of *35S*:*amiRNA PM-ANT1* lines 6 and 15 is unaltered when compared with the wild type. Alternatively, pollination of a wild-type pistil with pollen derived from heterozygous mutant lines 6 and 15 led to 54 and 89 kanamycin-resistant seedlings, respectively, and 49 and 63 kanamycin-sensitive seedlings (see Supplemental Table 1 online). The corresponding ratios are 52.9 and 58.6%, which also indicate intactness of the female gametophyte (see Supplemental Table 1 online). Control pollination by self-fertilization leads in both mutant lines to ~75% of kanamycin-resistant seedlings (see Supplemental Table 1 online), which is fully in line with the conclusion that both male and female gametophytes did not show altered properties when compared with the wild type.

Nuclear phenotypes and pollen morphology were further analyzed by 4′,6-diamidino-2-phenylindole (DAPI) and Alexander staining. DAPI staining revealed that pollen from all plant lines possess a larger diffusely stained vegetative nucleus and two stained sperm cell nuclei (see Supplemental Figures 3A to 3D online). Similarly, the morphology of wild-type and mutant pollen is identical as revealed by Alexander staining (see Supplemental Figures 3E to 3H online). To identify the origin of the decreased pollination efficiency observed in *35S*:*amiRNA PM-ANT1* lines 6 and 15, we analyzed the presence of pollen tubes in fully mature pistil tissues from wild-type and mutant lines. Interestingly, pistils from wild-type and mutant line 9 are characterized by the presence of many pollen tubes, as visualized by bright pollen tube staining with Aniline blue (see Supplemental Figures 3I and 3K online). By contrast, pistils from mutant lines 6 and 15 showed substantially reduced numbers of pollen tubes. In the style of mutant line 6, pollen tubes were not visible, and in the style from mutant line 15, only four to five individual pollen tubes were apparent (see Supplemental Figures 3J and 3L online).

Delayed Dehiscence of *35S*:*amiRNA PM-ANT1* Anthers

The fact that *PM-ANT1* is highly expressed in mature pollen grains (Figure 3; see Supplemental Figure 2 online) and the reduced silique development in *35S*:*amiRNA PM-ANT1* mutants (Figures 5B to 5F) provoked us to analyze the morphology of the corresponding flowers in more detail. Flowers from both the wild type and the three *35S*:*amiRNA PM-ANT1* lines developed with the same velocity, leading after 12 weeks to fully opened organs, possessing all structures required for pollination (Figures 7A to 7D). However, a closer look at the anther morphology revealed

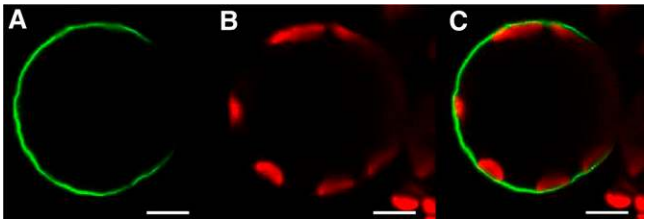

Figure 3. Subcelluar Localization of a C-Terminal PM-ANT1-GFP Fusion Protein in Tobacco Protoplasts.

Localization of the PM-ANT1-GFP fusion protein **(A)**, autofluorescence of chloroplasts **(B)**, and merge of **(A)** and **(B)** (in **[C]**) are given as single confocal plane images. Bars = 10 μm.

that *35S*:*amiRNA PM-ANT1* lines 6 and 15 exhibited impaired anther opening (Figures 7B and 7D), whereas anthers from the wild type and line 9 were fully opened and decorated with pollen grains (Figures 7A and 7C).

To determine whether impaired dehiscence was caused by a morphological abnormality of the anthers, we analyzed transverse sections of the representative mutant line 6 and wild-type anthers. About 3 d before flower opening, anthers from both the wild type and mutant line 6 were closed and harbored nearly fully developed pollen grains (Figures 7E and 7G). Furthermore, other cell structures associated with the anther, such as epidermis, endothecium, tapetum, stomium, and connective and vascular bundles, appeared to be normally developed. However, during progression of growth, wild-type anthers dehisced at the stomium and expelled the previously embedded pollen grains (Figure 7F), whereas anthers from *35S*:*amiRNA PM-ANT1* line 6 did not dehisce and thus did not provide the functional intact pollen grains (see Supplemental Table 1 online) at the anther surface, while the stigma was receptive for pollination (Figure 7H).

Altered ATP Levels in *35S*:*amiRNA PM-ANT1* Pollen

As demonstrated above, PM-ANT1-GFP resides in the plant plasma membrane, the corresponding gene is substantially expressed in pollen grains, and the carrier transports ATP after recombinant synthesis in *E. coli* (Figures 2 to 4). Thus, we tested whether pollen grains enriched from the wild type or *35S*:*amiRNA PM-ANT1* lines showed altered internal and external ATP levels. For this, we isolated pollen grains from the corresponding anthers, suspended them in germination medium, and quantified ATP in intact pollen grains and after exportation into the medium via Luciferase/Luciferin-induced luminescence.

Pollen grains from the wild type and *35S*:*amiRNA PM-ANT1* line 9 contained similar ATP levels, approaching ~39 pmol/μg protein (Figure 8A). By contrast, pollen cells from *35S*:*amiRNA PM-ANT1* lines 6 and 15 contained significantly increased internal ATP levels, namely, 60 pmol ATP/μg protein in pollen from mutant line 6 and 52 pmol ATP/μg protein in pollen from mutant line 15 (Figure 8A). Wild-type and mutant line 9 exported ATP at similar rates, approaching ~4.5 pmol ATP/μg protein in 5 min (Figure 8B). Interestingly, although the internal ATP concentration in pollen cells from mutant lines 6 and 15 was higher than in wild-type pollen (Figure 8A), the rates of ATP export into the germination medium were substantially decreased when compared with wild-type and mutant line 9 pollen cells. Pollen from mutant line 6 exported ~1.7 pmol ATP/μg protein within 5 min of incubation, and pollen from mutant line 15 exported only 2.2 pmol ATP/μg protein (Figure 8B).

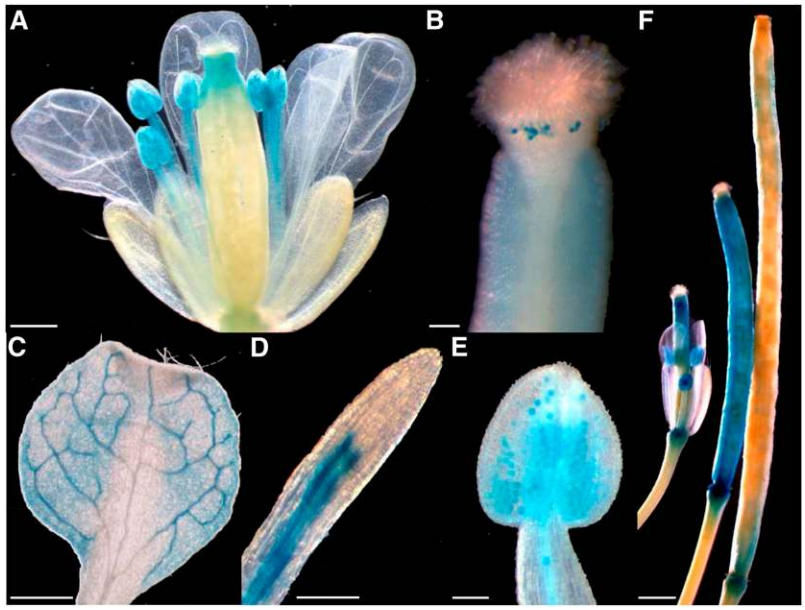

Figure 4. Histochemical Localization of *PM-ANT1* Gene Expression.

Flower **(A)**, pistil with pollen grains **(B)**, leaf of a 2-week-old plant **(C)**, root of a 2-week-old plant **(D)**, anther **(E)**, and developing and mature siliques **(F)**. Bars = 500 μm in **(A)**, 100 μm in **(B)**, 500 μm in **(C)**, 100 μm in **(D)** and **(E)**, and 1000 μm in **(F)**.

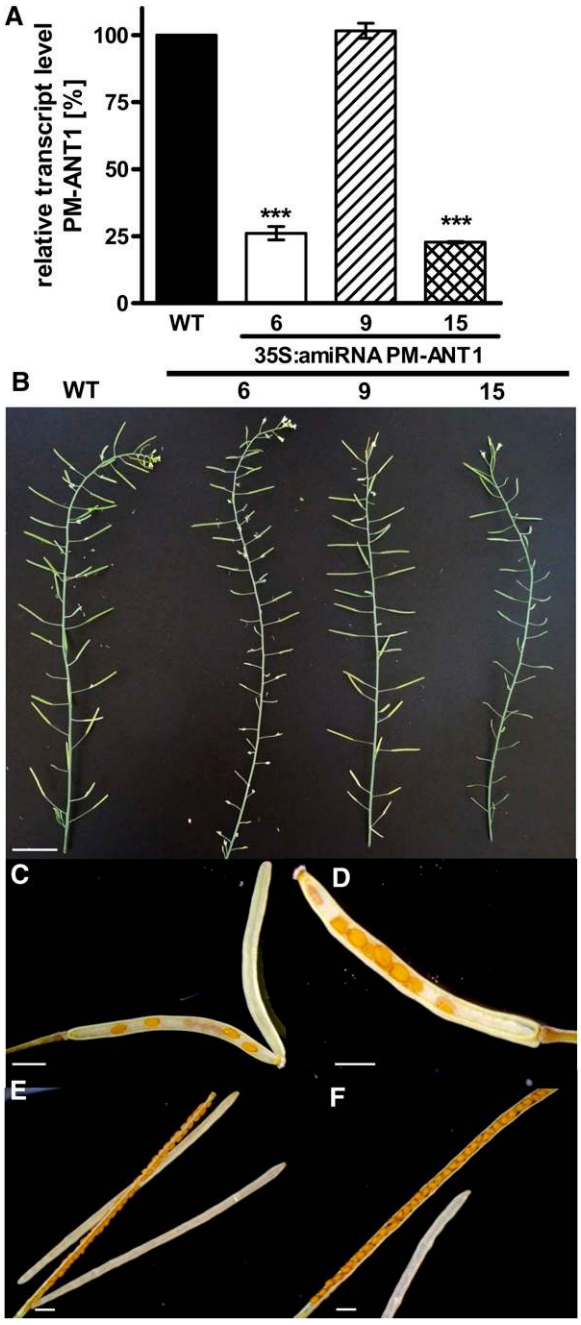

Figure 5. Phenotype of Wild-Type and *35S:amiRNA PM-ANT1* Lines.

Relative transcript level of *35S:amiRNA PM-ANT1* lines **(A)** and inflorescences of the wild type (WT) and three *35S:amiRNA PM-ANT1* lines **(B)**. Siliques of *35S:amiRNA PM-ANT1*-line 6 **(C)**, -line 15 **(D)**, -line 9 **(E)**, and the wild type **(F)**. All experiments were repeated at least three times with similar results. Data represent means ± SE. Asterisks report the significance level according to Student's *t* test. ***P < 0.001. Bars = 20 mm in **(B)** and 1 mm in **(C)** to **(F)**.

DISCUSSION

PM-ANT1 Is a Plasma Membrane–Located Adenylate Carrier

In plants, ATP is mainly regenerated in mitochondria and chloroplasts, but with the exception of vacuoles, virtually each organelle (Geigenberger et al., 2010) and the apoplast (Roux

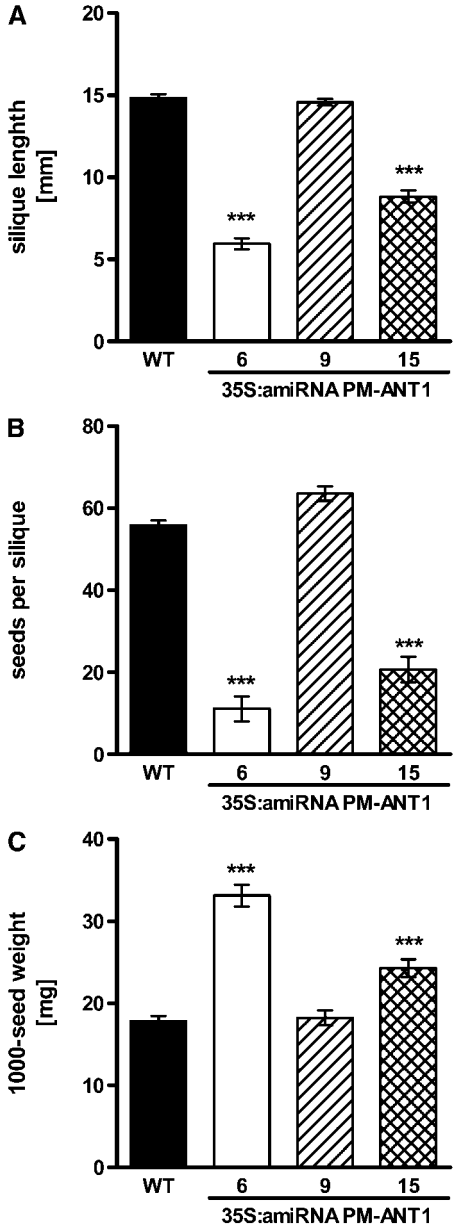

Figure 6. Seed and Silique Analysis in the Wild Type and *35S:amiRNA PM-ANT1* Mutants.

Silique length **(A)**, number of seeds per silique **(B)**, and 1000-seed weight **(C)** for the wild type (WT) and three independent *35S:amiRNA PM-ANT1*-lines. Data represent means ± SE of three independent experiments. Asterisks report the significance level according to Student's *t* test. ***P < 0.001.

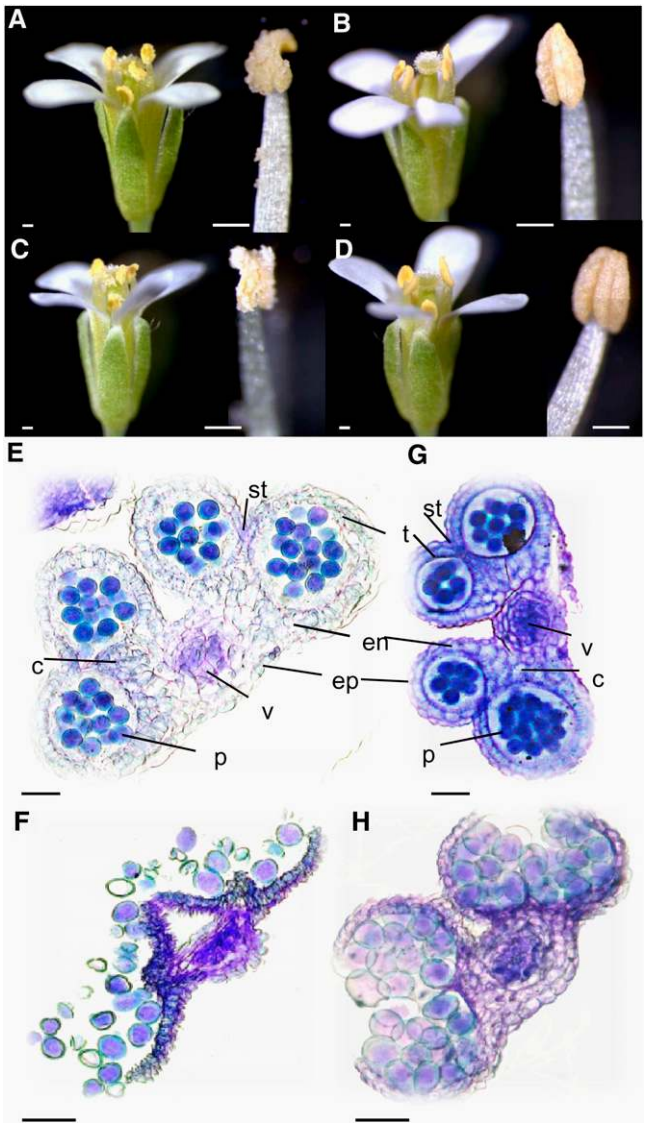

Figure 7. Flower and Anther Analysis of the Wild Type and *35S:amiRNA PM-ANT1*-Lines.

(A) to **(D)** Flowers immediately after opening and with anthers removed. The wild type **(A)**, *35S:amiRNA PM-ANT1*-line 6 **(B)**, -line 9 **(C)**, and -line 15 **(D)**.
(E) to **(H)** Transverse sections of anthers.
(E) Developing wild-type anther in a flower bud 3 d before opening. Epidermis (ep), endothecium (en), tapetum (t), stomium (st), connective (c), vascular bundle (v), and pollen grains (p).
(F) Dehisced wild-type anther of an open flower.
(G) Developing *35S:amiRNA PM-ANT1*-line 6 anther in a flower bud 3 d before opening.
(H) Undehisced *35S:amiRNA PM-ANT1*-line 6 anther of an open flower. Bars = 200 μm **(A)** to **(D)** and 40 μm in **(E)** to **(H)**.

and Steinebrunner, 2007) has to be provided with this metabolite. Due to the substantial molecular size of adenylates and due to the high charge of this class of molecules, corresponding membranes must harbor specific proteins that allow transport across this physical barrier. PM-ANT1 fulfils basic criteria required for ATP transporters as this protein exhibits high structural similarity to the well-characterized ADP/ATP carriers AAC1-3, which reside in the inner mitochondrial membrane (Figure 1; Haferkamp et al., 2002), shows three METS, and possess the highly conserved RRRMMM motif (Figure 1) critical for ATP transport (Nelson et al., 1993; Nelson and Douglas, 1993). Thus, it was not surprising to observe that PM-ANT1 transports adenylates (Figure 2C, Table 1) and fully legitimates the position of PM-ANT1 as one of five MCF-type ATP/ADP carriers encoded in the *Arabidopsis* genome (Picault et al., 2004).

Analysis of the PM-ANT1-GFP location (Figure 3), the colocalization of PM-ANT1-GFP and the plasma membrane–located PIP2a-mCherry (see Supplemental Figure 1 online), and the demonstration that pollen grains from *35S:amiRNA PM-ANT1* lines showed increased internal and decreased external ATP levels (Figures 8A and 8B) gave rise to the assumption that this transporter locates to the plasma membrane and that PM-ANT1 is functional in this cellular environment. Interestingly, the plasma

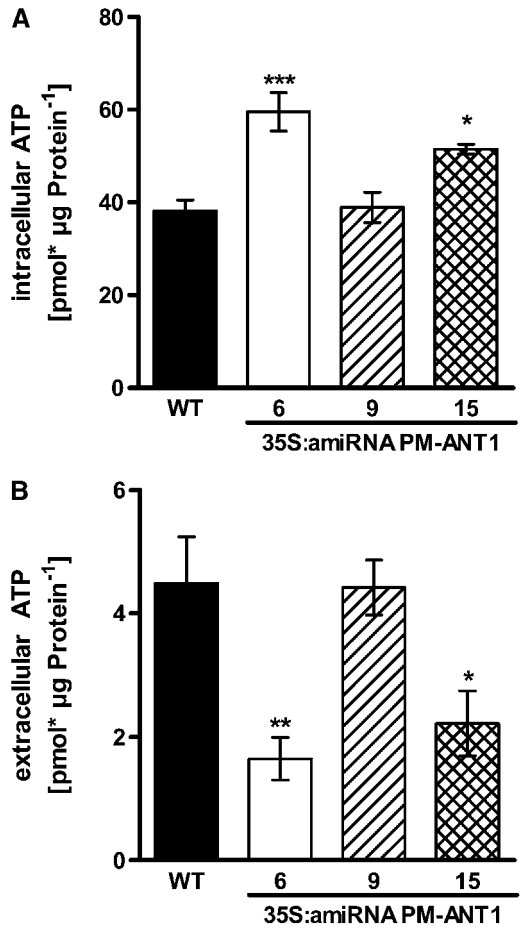

Figure 8. Pollen ATP Content of the Wild Type and *35S:amiRNA PM-ANT1* Lines.

Intracellular ATP levels **(A)** and extracellular ATP levels **(B)** after 5 min of incubation. Data represent means ± SE of three independent experiments. Asterisks indicate the significance level according to Student's *t* test: ***P < 0.001, **P < 0.01, and *P < 0.05.

membrane location of PM-ANT1 gains independent support by a recent proteomic study on this membrane, in which PM-ANT1 has been identified as an intrinsic protein (Mitra et al., 2009, and supplemental data therein). Thus, PM-ANT1 joins the rising number of MCF-type nucleotide carriers located in nonmitochondrial membranes like thylakoids, plastid envelopes, peroxisomes, glyoxysomes, and the ER (Leroch et al., 2005, 2008; Kirchberger et al., 2007, 2008; Thuswaldner et al., 2007).

Recombinant expression of PM-ANT1 allowed identification of the basic biochemical properties of this carrier. We observed that substrate specificity of PM-ANT1 is based on the number of phosphate moieties attached to the nucleoside, since monophosphate nucleotide derivates and nucleotide sugars do, in contrast with di- or triphosphates, hardly inhibit PM-ANT1–mediated ATP transport (Table 1). On the other hand, all RNA and DNA nucleotides presented acted as substantial inhibitors (Table 1), indicating that the substrate binding site of PM-ANT1 does not specify on the sugar domain of these metabolites. According to the lack on inhibition of PM-ANT1–mediated ATP transport by NAD^+ and derivatives thereof (Table 1), we would like to propose that this transporter is not involved in the release of this class of metabolite in the plant apoplast (Zhang and Mou, 2009).

Promotor-GUS analysis, confirmed by Genevestigator data, showed that the *PM-ANT1* gene is expressed in several *Arabidopsis* tissues and cell types. Inter alia, the abundance of *PM-ANT1* in pollen residing in anthers appears remarkable (Figure 4A; Zimmermann et al., 2004). In addition to pollen grains, we found *PM-ANT1* expression in veins from young leaves, root central cylinders, and young siliques. However, since we did not observe any obvious phenotypic changes in the latter tissues, we focused our attention on pollen and the properties of tissues connected to pollen development/function.

In plants and humans, different transport mechanisms have been proposed to increase extracellular ATP levels. Overexpression of the gene coding for the *Arabidopsis* ABC transporter PGP1 led to ATP accumulation on the plant leaf surfaces, and yeast cells overexpressing PGP1 showed increased extracellular ATP levels. These observations led to the proposal that PGP1 acts as a transporter required for extracellular ATP release in plants (Thomas et al., 2000). Interestingly, in animals, the existence of so far not identified plasma membrane-located MCF-type ATP carriers have already been proposed (Gatof and Fitz, 2005), and these carriers might act as alternatives to channels, ABC-type transporters, and vesicles (Thomas et al., 2000; Bodin and Burnstock, 2001b; Dutta et al., 2002; Lazarowski et al., 2003; Kim et al., 2006; Sawada et al., 2008).

The lack of transport inhibition by the presence of CCCP indicates that PM-ANT1–mediated ATP movement is independent upon an existing proton motif force and speaks for a facilitated diffusion. It seems possible that facilitated diffusion catalyzed by PM-ANT1 represents an important property for ATP release into the plant apoplast, since ATP export is then energized by an existing ATP gradient across this membrane. Usually, cytosolic ATP levels are high and reach concentrations of several millimolar (Stitt et al., 1989), but apoplastic ATP levels are in the micromolar range (Song et al., 2006), leading to a 100-fold concentration difference, which should suffice to drive ATP export. Moreover, facilitated diffusion would also prevent massive export of ATP into the apoplast where this compound is the subject of rapid hydrolysis to adenosine and phosphates (Riewe et al., 2008) by the concerted action of apoplastic apyrases (nucleoside triphosphate-diphosphohydrolases) and so far not identified AMP phosphatases (Wu et al., 2007). In line with this, we observed that PM-ANT1 exhibits a comparably low apparent affinity for ATP (Km 284 μM; Figure 2D). This value is similar to the apparent affinity of the other endomembrane-located ATP carrier ER-ANT1 (Leroch et al., 2008) but considerably lower than the affinity of all plant ATP transporters residing in peroxisomes, thylakoids, or plastid envelopes (Tjaden et al., 1998b; Thuswaldner et al., 2007; Linka et al., 2008).

PM-ANT1 Is Important for Anther Development

It is already known that extracellular ATP is critical for pollen function in respect to pollen germination and pollen tube growth (Steinebrunner et al., 2003; Reichler et al., 2009). Growing pollen tubes release ATP into the extracellular matrix where extracellular ATP levels correlate closely with regions of active growth and cell expansion. However, the observation that ATP release from growing pollen tubes is inhibited by Brefeldin A (Wang et al., 2005; Kim et al., 2006) indicates that this process is due to vesicular trafficking and not mediated by a plasma membrane–located ATP exporter like PM-ANT1 (Figure 3). Therefore, it is not surprising that pollen from wild-type and *35S:amiRNA PM-ANT1* lines exhibit the same fertility efficiency (see Supplemental Table 1 online), although impaired anther development undoubtedly leads to decreased silique lengths and reduced numbers of seeds per silique (Figures 6A and 6B). The latter alterations correlate with increased weight of the remaining fully developed seeds (Figure 6C). This effect is the result of the decreased sink capacity in mutant siliques (Figures 5C, 5D, and 6B) and unchanged size of the rosettes ultimately leading to the availability of more photosynthates for the remaining developing seed. This conclusion seems justified since recent data showed that stimulation or reduction of photosynthate supply to developing *Arabidopsis* seeds or to wheat (*Triticum aestivum*) grains provokes correspondingly altered organ biomasses (Weichert et al., 2010; Wingenter et al., 2010). Obviously, decreased *PM-ANT1* mRNA levels correlate with impaired anther development, which leads to fewer mutant seeds (Figures 6B, 7B, and 7C). Thus, it seems feasible that this close correlation prevents identification of amiRNA mutants with less than ~25% *PM-ANT1* mRNA levels (Figure 5A).

During pollen maturation the process of dehydration, which usually occurs just before anthesis, induces a state of metabolic quiescence that confers tolerance to upcoming environmental stresses (Lin and Dickinson, 1984). As ATP is the universal energy currency and is involved in most metabolic processes, export into the extracellular matrix may help to achieve metabolic quiescence and may simultaneously act as signaler to the surrounding anther tissues, leading to dehiscence and opening. In fact, such ATP-driven intercellular communication between different cell types is not an invention restricted to plants. For instance, in animals, microglia cells are attracted to sites of injury by glia cells after release of ATP (Samuels et al., 2010), and in human brains, glia cells release ATP to communicate with

neighboring neurons (Bodin and Burnstock, 2001b; Kumaria et al., 2008). Without success, we tried to rescue the transport defect in *35S:amiRNA PM-ANT1* lines 6 and 15 by spraying different types of nucleotides onto developing flowers. However, both the pollen grains per se and the tapetum, representing the innermost anther cell layer, are completely covered with lipid-derived waxes (Piffanelli et al., 1997; Jung et al., 2006), representing a well-characterized physical barrier for highly charged solutes.

In summary, PM-ANT1 is an MCF-type transporter located at the plasma membrane of a eukaryotic cell. The activity of PM-ANT1 is not required for pollen viability per se but is critical for pollination efficiency as the complex process of dehiscence is distorted in amiRNA mutants, which exhibit reduced activity. Similar to animals, in which channels, ABC-type carriers, and vesicles have been described as mechanisms for ATP export, plants seem to possess various mechanisms that allow cellular export of ATP as a signaling compound. The molecular characterization of PM-ANT1 provides further insight into the remarkably wide subcellular location and physiological implication of MCF-type carriers in plants.

METHODS

Cultivation of Plants

Wild-type and transgenic *Arabidopsis thaliana* plants (ecotype Columbia-0) were used. Prior to germination, seeds were imbibed for 24 h in the dark at 4°C (Weigel and Glazebrook, 2002), in standardized ED73 soil. Plant growth was performed at 22°C in a 10-h-light/14-h-dark climate-controlled chamber (Percival growth chambers; CLF Plant Climatics). After development of a leaf rosette (~4 to 5 cm), the light phase was prolonged (16-h-light/day) to induce flowering until the life cycle was completed.

Construction of the Sequence Alignment

Multiple alignments of protein sequences were performed with the program ClustalX (Thompson et al., 1997).

Transient Expression of a *PM-ANT1-GFP* Fusion Construct

To construct PM-ANT1-GFP fusion proteins, the coding region of *PM-ANT1* was amplified by PCR on first-strand cDNA from *Arabidopsis* leaf tissues and inserted in frame with the GFP coding region of the vector pGFP2 (Kost et al., 1998) using the primers PM-ANT1_gfp_for and PM-ANT1_gfp_rev (see Supplemental Table 2 online). Protoplasts isolated from sterile-grown tobacco (*Nicotiana tabacum* cv W38) were transformed with column-purified plasmid DNA (30 mg/1.5*10^6 cells; Wendt et al., 2000). After 24 h of incubation at 24°C in the dark, protoplasts were analyzed for the presence of green fluorescence using a Leica TCS SP5II confocal microscope system. GFP was excited at 488 nm, and the emission was detected at 505 to 540 nm using a ×63 water objective.

Heterologous Expression of PM-ANT1 in *Escherichia coli*

To construct *E. coli* plasmids expressing PM-ANT1 with a N-terminal His tag, the coding region of *PM-ANT1* was amplified by PCR on first-strand cDNA from *Arabidopsis* leaf tissues and introduced into the IPTG-inducible expression vector pET16b (Novagen) using the primers PM-ANT1_pet16b_for and PM-ANT1_pet16b_rev (see Supplemental Table 2 online). The *E. coli* strain Rosetta 2 (pLysS; Novagen) was exploited for heterologous synthesis. Uptake experiments with *E. coli* cells after synthesis of PM-ANT1 were performed as described earlier (Haferkamp et al., 2002; Leroch et al., 2005). SDS-PAGE was performed as described earlier (Laemmli 1970) and stained with Coomassie Brillant Blue R 250 or used for immunoblots.

Staining for GUS Activity

For the histochemical localization of promoter activity, a 1259-bp promoter region of *PM-ANT1* was amplified by PCR on genomic DNA and inserted upstream of the GUS gene of pGPTV (Becker et al., 1992) using the primers PM-ANT1_gus_for and PM-ANT1_gus_rev (see Supplemental Table 2 online). The resulting construct was transformed in the *Agrobacterium tumefaciens* strain GV3101. Transformation of *Arabidopsis* was conducted according to the floral-dip method (Clough and Bent, 1998). Tissue from transgenic plants was collected in glass vials previously loaded with ice-cold 90% acetone and incubated for 20 min at room temperature. Subsequently, the samples were stained according to standard protocols (Weigel and Glazebrook, 2002).

Cloning of *35S:amiRNA PM-ANT1*

A suitable target site for the microRNA was identified by following the instructions on http://wmd2.weigelworld.org. The *35S:amiRNA PM-ANT1* construct was cloned according to the protocol as described by Schwab et al. (2006) with minor changes. Primer sequences are listed in Supplemental Table 2 online. The PCR amplification product, including the specific amiRNA, was subsequently cloned into the pA35S vector and finally into the plant transformation vector pCambia 2200 (Hajdukiewicz et al., 1994). Transformation of *Arabidopsis* was conducted according to the floral-dip method (Clough and Bent, 1998). Transgenic plants were selected based on kanamycin resistance conferred by the nptII gene present in pCambia 2200.

Quantitative Real-Time RT-PCR

Total RNA was prepared from *Arabidopsis* leaf tissues using the RNeasy Plant Mini Kit (Qiagen). To remove any contaminating DNA, the samples were treated with DNase (RNase-free DNase Kit; Qiagen). Quantitative PCR was performed using MyIQ-Cycler (Bio-Rad) and IQ SYBR Green Supermix (Bio-Rad) according to the manufacturer's instructions with the following cycler conditions: 20 min at 50°C, 15 min at 95°C, and 55 cycles of 15 s at 95°C, 25 s at 58°C, and 40 s at 72°C. The gene-specific oligonucleotides used for real-time RT-PCR are listed in Supplemental Table 2 online. The elongation factor EF-1α was used for quantitative normalization (Curie et al., 1991).

Microscopy

For observation of anther transverse sections, flower buds were embedded in Technovit 7100 (Heraeus-Kulzer) according to user instructions. Ten-micrometer sections were prepared and stained with 0.5% Toluidine blue. Images were acquired using a Cannon PowerShot G5 camera coupled to a Zeiss Axioskop 50 microscope. All other images were acquired using a Leica DFC 420C camera coupled to a Leica MZ10F stereomicroscope.

ATP Quantification

For quantification of intra- and extracellular ATP levels, pollen were isolated essentially as described (Boavida and McCormick, 2007). Therefore, 60 freshly opened flowers were collected in germination medium and agitated briefly by shaking. Then, the flower parts were removed with a pair of forceps, and the pollen grains were pelleted for 30 s at 800*g* and

resuspended with 100 μL fresh germination medium. Pollen grains in 20 μL suspension were disrupted by ultrasound and used for protein quantification (Bradford, 1976). For intracellular ATP measurement, another 20 μL of the pollen suspension was used, and for extracellular ATP measurement, the pollen grains were incubated for 5 min and pelleted and 50 μL of the supernatant was used for further processing. To avoid metabolic degradation of ATP, the samples were subsequently treated with buffer A (7% perchloric acid and 10 mM EDTA) and buffer B (5 M KOH and 1 M triethanolamine) as described (Stitt et al., 1989). The resulting supernatant was diluted with 50 mM Tris-HCl, pH 8.0, and ATP was measured by ENLITEN rLuciferase/Luciferin reagent (Promega) according to user instructions. Luminescence was measured using a Tecan Infinite M200 multimode microplate reader equipped with an injector. For measurements, a 1-s delay time after rLuciferase/Luciferin reagent injection and 10-s relative light unit signal integration time were used.

Accession Numbers

Sequence data from this article can be found in the Arabidopsis Genome Initiative or GenBank/EMBL databases under the following accession numbers: PM-ANT1 (At5g56450), ER-ANT1 (At5g17400), AAC1 (At3g08580), AAC2 (At5g13490), AAC3 (At4g28390), and EF1α (At5g60390).

Supplemental Data

The following materials are available in the online version of this article.

Supplemental Figure 1. Colocalization of a C-Terminal PM-ANT1-GFP Fusion Protein with the *Arabidopsis* Plasma Membrane Aquaporin PIP2a-mcherry in Tobacco Protoplasts.

Supplemental Figure 2. Relative Expression of *PM-ANT1* during Pollen Development.

Supplemental Figure 3. Pollen Analysis of Wild-Type and *35S*:*amiRNA PM-ANT1* Lines.

Supplemental Table 1. Segregation Analysis of *35S*:*amiRNA PM-ANT1*.

Supplemental Table 2. Primers Used for Cloning and Quantitative Real-Time PCR.

ACKNOWLEDGMENTS

Work in the lab of H.E.N. was financially supported by the Deutsche Forschungsgemeinschaft (Reinhart Koselleck Grant) and by the Federal State of Rheinland Pfalz (Research Initiative Membrane Proteins). We thank Simon Kirchberger and Michaela Leroch (University of Kaiserslautern) for supporting the creation of artificial microRNA and GUS plants and Garvin Meißner (University of Kaiserslautern) for helping with the seed and silique analysis.

Received February 21, 2011; revised, March 28, 2011; accepted April 11, 2011; published May 3, 2011.

REFERENCES

Alonso, J.M., et al. (2003). Genome-wide insertional mutagenesis of *Arabidopsis thaliana*. Science **301:** 653–657.

Arai, Y., Hayashi, M., and Nishimura, M. (2008). Proteomic identification and characterization of a novel peroxisomal adenine nucleotide transporter supplying ATP for fatty acid beta-oxidation in soybean and *Arabidopsis*. Plant Cell **20:** 3227–3240.

Ast, M., Gruber, A., Schmitz-Esser, S., Neuhaus, H.E., Kroth, P.G., Horn, M., and Haferkamp, I. (2009). Diatom plastids depend on nucleotide import from the cytosol. Proc. Natl. Acad. Sci. USA **106:** 3621–3626.

Becker, D., Kemper, E., Schell, J., and Masterson, R. (1992). New plant binary vectors with selectable markers located proximal to the left T-DNA border. Plant Mol. Biol. **20:** 1195–1197.

Boavida, L.C., and McCormick, S. (2007). Temperature as a determinant factor for increased and reproducible in vitro pollen germination in *Arabidopsis thaliana*. Plant J. **52:** 570–582.

Bodin, P., and Burnstock, G. (2001a). Evidence that release of adenosine triphosphate from endothelial cells during increased shear stress is vesicular. J. Cardiovasc. Pharmacol. **38:** 900–908.

Bodin, P., and Burnstock, G. (2001b). Purinergic signalling: ATP release. Neurochem. Res. **26:** 959–969.

Bradford, M.M. (1976). A rapid and sensitive method for the quantification of microgram quantities of protein utilizing the principle of protein-dye binding. Anal. Biochem. **72:** 248–254.

Claros, M.G., and Vincens, P. (1996). Computational method to predict mitochondrially imported proteins and their targeting sequences. Eur. J. Biochem. **241:** 779–786.

Clough, S.J., and Bent, A.F. (1998). Floral dip: A simplified method for *Agrobacterium*-mediated transformation of *Arabidopsis thaliana*. Plant J. **16:** 735–743.

Curie, C., Liboz, T., Bardet, C., Gander, E., Médale, C., Axelos, M., and Lescure, B. (1991). Cis and trans-acting elements involved in the activation of *Arabidopsis thaliana* A1 gene encoding the translation elongation factor EF-1 alpha. Nucleic Acids Res. **19:** 1305–1310.

Dutta, A.K., Okada, Y., and Sabirov, R.Z. (2002). Regulation of an ATP-conductive large-conductance anion channel and swelling-induced ATP release by arachidonic acid. J. Physiol. **542:** 803–816.

Emanuelsson, O., Nielsen, H., Brunak, S., and von Heijne, G. (2000). Predicting subcellular localization of proteins based on their N-terminal amino acid sequence. J. Mol. Biol. **300:** 1005–1016.

Gatof, D., and Fitz, J. (2005). Extracellular ATP: Important developments in purinergic signaling. In Signaling Pathways in Liver Diseases, J.F. Dufour, P.A. Clavien, and C.G.R. Trautwein, eds (Heidelberg, Germany: Springer), pp. 201–210.

Geigenberger, P., Riewe, D., and Fernie, A.R. (2010). The central regulation of plant physiology by adenylates. Trends Plant Sci. **15:** 98–105.

Haferkamp, I., Hackstein, J.H., Voncken, F.G., Schmit, G., and Tjaden, J. (2002). Functional integration of mitochondrial and hydrogenosomal ADP/ATP carriers in the *Escherichia coli* membrane reveals different biochemical characteristics for plants, mammals and anaerobic chytrids. Eur. J. Biochem. **269:** 3172–3181.

Hajdukiewicz, P., Svab, Z., and Maliga, P. (1994). The small, versatile pPZP family of Agrobacterium binary vectors for plant transformation. Plant Mol. Biol. **25:** 989–994.

Hardie, D.G., Carling, D., and Carlson, M. (1998). The AMP-activated/SNF1 protein kinase subfamily: Metabolic sensors of the eukaryotic cell? Annu. Rev. Biochem. **67:** 821–855.

Honys, D., and Twell, D. (2004). Transcriptome analysis of haploid male gametophyte development in *Arabidopsis.* Genome Biol. **5:** R85.

Jung, K.H., Han, M.J., Lee, D.Y., Lee, Y.S., Schreiber, L., Franke, R., Faust, A., Yephremov, A., Saedler, H., Kim, Y.W., Hwang, I., and An, G. (2006). Wax-deficient anther1 is involved in cuticle and wax production in rice anther walls and is required for pollen development. Plant Cell **18:** 3015–3032.

Kampfenkel, K., Möhlmann, T., Batz, O., Van Montagu, M., Inzé, D., and Neuhaus, H.E. (1995). Molecular characterization of an *Arabidopsis thaliana* cDNA encoding a novel putative adenylate translocator of higher plants. FEBS Lett. **374:** 351–355.

Kim, S.Y., Sivaguru, M., and Stacey, G. (2006). Extracellular ATP in plants. Visualization, localization, and analysis of physiological significance in growth and signaling. Plant Physiol. **142:** 984–992.

Kirchberger, S., Leroch, M., Huynen, M.A., Wahl, M., Neuhaus, H.E., and Tjaden, J. (2007). Molecular and biochemical analysis of the plastidic ADP-glucose transporter (ZmBT1) from *Zea mays*. J. Biol. Chem. **282:** 22481–22491.

Kirchberger, S., Tjaden, J., and Neuhaus, H.E. (2008). Characterization of the Arabidopsis Brittle1 transport protein and impact of reduced activity on plant metabolism. Plant J. **56:** 51–63.

Klingenberg, M. (2008). The ADP and ATP transport in mitochondria and its carrier. Biochim. Biophys. Acta **1778:** 1978–2021.

Kost, B., Spielhofer, P., and Chua, N.-H. (1998). A GFP-mouse talin fusion protein labels plant actin filaments in vivo and visualizes the actin cytoskeleton in growing pollen tubes. Plant J. **16:** 393–401.

Kumaria, A., Tolias, C.M., and Burnstock, G. (2008). ATP signalling in epilepsy. Purinergic Signal. **4:** 339–346.

Laemmli, U.K. (1970). Cleavage of structural proteins during the assembly of the head of bacteriophage T4. Nature **227:** 680–685.

Lazarowski, E.R., Boucher, R.C., and Harden, T.K. (2003). Mechanisms of release of nucleotides and integration of their action as P2X- and P2Y-receptor activating molecules. Mol. Pharmacol. **64:** 785–795.

Leroch, M., Kirchberger, S., Haferkamp, I., Wahl, M., Neuhaus, H.E., and Tjaden, J. (2005). Identification and characterization of a novel plastidic adenine nucleotide uniporter from *Solanum tuberosum*. J. Biol. Chem. **280:** 17992–18000.

Leroch, M., Neuhaus, H.E., Kirchberger, S., Zimmermann, S., Melzer, M., Gerhold, J., and Tjaden, J. (2008). Identification of a novel adenine nucleotide transporter in the endoplasmic reticulum of *Arabidopsis*. Plant Cell **20:** 438–451.

Lin, J.J., and Dickinson, D.B. (1984). Ability of pollen to germinate prior to anthesis and effect of desiccation on germination. Plant Physiol. **74:** 746–748.

Linka, N., Theodoulou, F.L., Haslam, R.P., Linka, M., Napier, J.A., Neuhaus, H.E., and Weber, A.P. (2008). Peroxisomal ATP import is essential for seedling development in *Arabidopsis thaliana*. Plant Cell **20:** 3241–3257.

Millar, A.H., and Heazlewood, J.L. (2003). Genomic and proteomic analysis of mitochondrial carrier proteins in Arabidopsis. Plant Physiol. **131:** 443–453.

Mitra, S.K., Walters, B.T., Clouse, S.D., and Goshe, M.B. (2009). An efficient organic solvent based extraction method for the proteomic analysis of Arabidopsis plasma membranes. J. Proteome Res. **8:** 2752–2767.

Möhlmann, T., Tjaden, J., Schwöppe, C., Winkler, H.H., Kampfenkel, K., and Neuhaus, H.E. (1998). Occurrence of two plastidic ATP/ADP transporters in *Arabidopsis thaliana* L.—Molecular characterisation and comparative structural analysis of similar ATP/ADP translocators from plastids and *Rickettsia prowazekii*. Eur. J. Biochem. **252:** 353–359.

Murcha, M.W., Millar, A.H., and Whelan, J. (2005). The N-terminal cleavable extension of plant carrier proteins is responsible for efficient insertion into the inner mitochondrial membrane. J. Mol. Biol. **351:** 16–25.

Nelson, D.R., and Douglas, M.G. (1993). Function-based mapping of the yeast mitochondrial ADP/ATP translocator by selection for second site revertants. J. Mol. Biol. **230:** 1171–1182.

Nelson, D.R., Lawson, J.E., Klingenberg, M., and Douglas, M.G. (1993). Site-directed mutagenesis of the yeast mitochondrial ADP/ATP translocator. Six arginines and one lysine are essential. J. Mol. Biol. **230:** 1159–1170.

Neuhaus, H.E., Batz, O., Thom, E., and Scheibe, R. (1993b). Purification of highly intact plastids from various heterotrophic plant tissues: Analysis of enzymic equipment and precursor dependency for starch biosynthesis. Biochem. J. **296:** 395–401.

Neuhaus, H.E., Henrichs, G., and Scheibe, R. (1993a). Characterization of glucose-6-phosphate incorporation into starch by isolated intact cauliflower-bud plastids. Plant Physiol. **101:** 573–578.

Nielsen, H., Engelbrecht, J., Brunak, S., and von Heijne, G. (1997). A neural network method for identification of prokaryotic and eukaryotic signal peptides and prediction of their cleavage sites. Int. J. Neural Syst. **8:** 581–599.

Palmieri, F., Pierri, C.L., De Grassi, A., Nunes-Nesi, A., and Fernie, A.R. (2011). Evolution, structure and function of mitochondrial carriers: A review with new insights. Plant J. **66:** 161–181.

Pebay-Peyroula, E., Dahout-Gonzalez, C., Kahn, R., Trézéguet, V., Lauquin, G.J., and Brandolin, G. (2003). Structure of mitochondrial ADP/ATP carrier in complex with carboxyatractyloside. Nature **6:** 39–44.

Pellegatti, P., Raffaghello, L., Bianchi, G., Piccardi, F., Pistoia, V., and Di Virgilio, F. (2008). Increased level of extracellular ATP at tumor sites: In vivo imaging with plasma membrane luciferase. PLoS ONE **3:** e2599.

Picault, N., Hodges, M., Palmieri, L., and Palmieri, F. (2004). The growing family of mitochondrial carriers in Arabidopsis. Trends Plant Sci. **9:** 138–146.

Piffanelli, P., Ross, J.H., and Murphy, D.J. (1997). Intra- and extracellular lipid composition and associated gene expression patterns during pollen development in *Brassica napus*. Plant J. **11:** 549–562.

Reichler, S.A., Torres, J., Rivera, A.L., Cintolesi, V.A., Clark, G., and Roux, S.J. (2009). Intersection of two signalling pathways: Extracellular nucleotides regulate pollen germination and pollen tube growth via nitric oxide. J. Exp. Bot. **60:** 2129–2138.

Reinhold, T., Alawady, A., Grimm, B., Beran, K.C., Jahns, P., Conrath, U., Bauer, J., Reiser, J., Melzer, M., Jeblick, W., and Neuhaus, H.E. (2007). Limitation of nocturnal import of ATP into Arabidopsis chloroplasts leads to photooxidative damage. Plant J. **50:** 293–304.

Reiser, J., Linka, N., Lemke, L., Jeblick, W., and Neuhaus, H.E. (2004). Molecular physiological analysis of the two plastidic ATP/ADP transporters from Arabidopsis. Plant Physiol. **136:** 3524–3536.

Riewe, D., Grosman, L., Fernie, A.R., Wucke, C., and Geigenberger, P. (2008). The potato-specific apyrase is apoplastically localized and has influence on gene expression, growth, and development. Plant Physiol. **147:** 1092–1109.

Roux, S.J., and Steinebrunner, I. (2007). Extracellular ATP: An unexpected role as a signaler in plants. Trends Plant Sci. **12:** 522–527.

Samuels, S.E., Lipitz, J.B., Dahl, G., and Muller, K.J. (2010). Neuroglial ATP release through innexin channels controls microglial cell movement to a nerve injury. J. Gen. Physiol. **136:** 425–442.

Saraste, M., and Walker, J.E. (1982). Internal sequence repeats and the path of polypeptide in mitochondrial ADP/ATP translocase. FEBS Lett. **144:** 250–254.

Sawada, K., Echigo, N., Juge, N., Miyaji, T., Otsuka, M., Omote, H., Yamamoto, A., and Moriyama, Y. (2008). Identification of a vesicular nucleotide transporter. Proc. Natl. Acad. Sci. USA **105:** 5683–5686.

Schmitz-Esser, S., Linka, N., Collingro, A., Beier, C.L., Neuhaus, H.E., Wagner, M., and Horn, M. (2004). ATP/ADP translocases: A common feature of obligate intracellular amoebal symbionts related to Chlamydiae and Rickettsiae. J. Bacteriol. **186:** 683–691.

Schwab, R., Ossowski, S., Riester, M., Warthmann, N., and Weigel, D. (2006). Highly specific gene silencing by artificial microRNAs in *Arabidopsis*. Plant Cell **18:** 1121–1133.

Song, C.J., Steinebrunner, I., Wang, X., Stout, S.C., and Roux, S.J. (2006). Extracellular ATP induces the accumulation of superoxide via NADPH oxidases in Arabidopsis. Plant Physiol. **140:** 1222–1232.

Stagg, J., and Smyth, M.J. (2010). Extracellular adenosine triphosphate and adenosine in cancer. Oncogene **29:** 5346–5358.

Steinebrunner, I., Wu, J., Sun, Y., Corbett, A., and Roux, S.J. (2003). Disruption of apyrases inhibits pollen germination in Arabidopsis. Plant Physiol. **131:** 1638–1647.

Stitt, M., Mc, C., Lilley, R., Gerhardt, R., and Heldt, H.W. (1989). Metabolite levels in specific cells and subcellular compartments of plant leaves. Methods Enzymol. **174:** 518–552.

Tang, W., Brady, S.R., Sun, Y., Muday, G.K., and Roux, S.J. (2003). Extracellular ATP inhibits root gravitropism at concentrations that inhibit polar auxin transport. Plant Physiol. **131:** 147–154.

Thomas, C., Rajagopal, A., Windsor, B., Dudler, R., Lloyd, A., and Roux, S.J. (2000). A role for ectophosphatase in xenobiotic resistance. Plant Cell **12:** 519–533.

Thompson, J.D., Gibson, T.J., Plewniak, F., Jeanmougin, F., and Higgins, D.G. (1997). The CLUSTAL_X windows interface: Flexible strategies for multiple sequence alignment aided by quality analysis tools. Nucleic Acids Res. **25:** 4876–4882.

Thuswaldner, S., Lagerstedt, J.O., Rojas-Stütz, M., Bouhidel, K., Der, C., Leborgne-Castel, N., Mishra, A., Marty, F., Schoefs, B., Adamska, I., Persson, B.L., and Spetea, C. (2007). Identification, expression, and functional analyses of a thylakoid ATP/ADP carrier from Arabidopsis. J. Biol. Chem. **282:** 8848–8859.

Tjaden, J., Möhlmann, T., Kampfenkel, K., Henrichs, G., and Neuhaus, H.E. (1998a). Altered plastidic ATP/ADP-transporter activity influences potato (*Solanum tuberosum*) tuber morphology, yield and composition of tuber starch. Plant J. **16:** 531–540.

Tjaden, J., Schwöppe, C., Möhlmann, T., Quick, P.W., and Neuhaus, H.E. (1998b). Expression of a plastidic ATP/ADP transporter gene in *Escherichia coli* leads to a functional adenine nucleotide transport system in the bacterial cytoplasmic membrane. J. Biol. Chem. **273:** 9630–9636.

Trautmann, A. (2009). Extracellular ATP in the immune system: More than just a "danger signal". Sci. Signal. **2:** pe6.

Wang, Q., Kong, L., Hao, H., Wang, X., Lin, J., Samaj, J., and Baluska, F. (2005). Effects of brefeldin A on pollen germination and tube growth. Antagonistic effects on endocytosis and secretion. Plant Physiol. **139:** 1692–1703.

Weichert, N., et al. (2010). Increasing sucrose uptake capacity of wheat grains stimulates storage protein synthesis. Plant Physiol. **152:** 698–710.

Weigel, D., and Glazebrook, J. (2002). Arabidopsis. A Laboratory Manual. (Cold Spring Harbor, NY: Cold Spring Harbor Laboratory Press).

Wendt, U.K., Wenderoth, I., Tegeler, A., and Von Schaewen, A. (2000). Molecular characterization of a novel glucose-6-phosphate dehydrogenase from potato (*Solanum tuberosum* L.). Plant J. **23:** 723–733.

Wingenter, K., Schulz, A., Wormit, A., Wic, S., Trentmann, O., Hoermiller, I.I., Heyer, A.G., Marten, I., Hedrich, R., and Neuhaus, H.E. (2010). Increased activity of the vacuolar monosaccharide transporter TMT1 alters cellular sugar partitioning, sugar signaling, and seed yield in Arabidopsis. Plant Physiol. **154:** 665–677.

Wu, J., Steinebrunner, I., Sun, Y., Butterfield, T., Torres, J., Arnold, D., Gonzalez, A., Jacob, F., Reichler, S., and Roux, S.J. (2007). Apyrases (nucleoside triphosphate-diphosphohydrolases) play a key role in growth control in Arabidopsis. Plant Physiol. **144:** 961–975.

Xing, S., and Zachgo, S. (2007). Pollen lethality: A phenomenon in Arabidopsis RNA interference plants. Plant Physiol. **145:** 330–333.

Zhang, X., and Mou, Z. (2009). Extracellular pyridine nucleotides induce PR gene expression and disease resistance in Arabidopsis. Plant J. **57:** 302–312.

Zimmermann, P., Hirsch-Hoffmann, M., Hennig, L., and Gruissem, W. (2004). GENEVESTIGATOR. Arabidopsis microarray database and analysis toolbox. Plant Physiol. **136:** 2621–2632.

Zybailov, B., Rutschow, H., Friso, G., Rudella, A., Emanuelsson, O., Sun, Q., and van Wijk, K.J. (2008). Sorting signals, N-terminal modifications and abundance of the chloroplast proteome. PLoS ONE **3:** e1994.